622. Damage detection of truss structure based on the variation in axial stress and strain energy predicted from incomplete measurements

Eun-Taik Lee[1], Hee-Chang Eun[2], Tae-Wan Kim[3]

[1] Department of Architectural Engineering, Chung-Ang University

[2] Department of Architectural Engineering, Kangwon National University

E-mail: *heechang@kangwon.ac.kr*

Tel.: 82-33-250-6223

Fax: 82-33-250-6211

[3] Department of Architectural Engineering, Kangwon National University

(Received 18 November 2010; accepted 15 May 2011)

Abstract. This study derives the static equilibrium equation of a damaged system on the basis of stiffness change due to damage as well as the constraint forces at measurements required for obtaining the measured data. Based on the derived equations, this work provides an analytical method to detect damage from the stress and strain energy variations between intact and damaged truss structures. The applicability of the proposed method is evaluated in detecting multiple damages of low rate in the truss structure from measured data contaminated by external noise. It is demonstrated that it is possible to properly detect damage in an isolated substructure by partitioning the damage-expected substructure from an entire structure and using the displacements measured at the boundary of the partitioned subsystem. The partitioning method has the benefits in reducing the computational time and measured data as well as improving the effectiveness of the damage detection process.

Keywords: truss, damage detection, static data, constraint, constraint force, equilibrium equation, structural partitioning.

1. Introduction

Regular inspection and condition assessment of civil structures are necessary to allow early detection of any damage and to enable maintenance and repair works at the initial damage phase so that the structural safety and reliability are guaranteed with minimal costs. Structural damage detection technique indicates the problem of how to locate and detect damage that occurred in a structure by using the observed changes of its dynamic and static characteristics. The structural identification can be used for structural health monitoring and damage assessment in a non-destructive way by tracking changes in relevant structural parameters. Damage detection techniques are realized by collecting necessary data by means of both experimental and numerical approaches as well as comparing and analyzing the difference between the undamaged and damaged states.

Structural health monitoring has been receiving a growing amount of interest from researchers in diverse fields of engineering. Many methods for improved serviceability of structures have been developed for the non-destructive techniques with the advent of various kinds of measuring systems and there have been a lot of analytical algorithms for damage detection. The damage identification methods are classified into two major categories: the dynamic identification methods using dynamic test data, and the static methods using static test data. The dynamic response of a real structure can be experimentally measured and compared with that computed mathematically. In cases of simple structural systems static tests are easily executable without any information of masses and damping ratios unlike dynamic approaches. Compared with the static identification techniques, the dynamic ones have been developed more maturely and the associated literature is fairly extensive. The static methods have attracted much attention because the accurate deformation or strain of the structure can be obtained rapidly and economically.

There have been a few studies on system identification using measured static data. Sheena et al. [1] presented an analytical method to assess the stiffness matrix by minimizing the difference between the actual and analytical stiffness matrices subjected to measured displacement constraints. Minimizing the difference between the applied and the internal forces, Sanayei and Scampoli [2] presented a finite element method for static parameter identification of structures by the systematic identification of plate-bending stiffness parameters for a one-third scale, reinforced-concrete pier-deck model. Sanayei and Onipede [3] provided an analytical method to identify the properties of structural elements from static test data such as a set of applied static forces and another set of measured displacements. Minimizing an index of discrepancy between the model and the measurements, Banan et al. [4], [5] proposed the mathematical formulations of two least-squares parameter estimators that evaluate element constitutive parameters of a finite-element model that corresponds to a real structural system from measured static response to a given set of loads. And they investigated the performance of the force-error estimator and the displacement-error estimator.

Cui et al. [6] developed a damage detection algorithm based on static displacement and strain. This method has a difficulty in requiring sufficient measurement information and load cases. The problem to identify concentrated cracks in Euler-Bernoulli beams has been considered based on displacement measurements available by the static tests [7], [8]. Wang et al. [9] presented a structural damage identification algorithm using static test and changes in natural frequencies. They presented improved damage signature matching technique to detect damage in the structure and an iterative estimation scheme to predict the damage extent. Bakhtiari-Nejad et al. [10] provided a method for detecting damage based on stored strain energy in elements and changes in the static responses of a structure. Caddemi and Morassi [11] handled an identification method for detecting a single crack in a beam based on the damage-induced variations in the static deflection of the beam. Choi et al. [12] considered a system identification technique using an elastic damage load theorem. Escobar et al. [13] proposed a damage detection method for locating and estimating structural damage of analytical building models using geometrical transformation matrix.

Rodriguez et al. [14] presented damage submatrices method (DSM) that localizes and assess degradation of stiffness at any structural element in a building. And they presented an approach to expand the condensed stiffness matrix of the damaged structure to global coordinates and to identify the damage. Ozgen and Kim [15] developed analytical methods to expand the experimental damping matrix to the size of the analytical model. Decoupling problem can be considered as the reverse of the substructuring problem. Starting from the known dynamic behavior of the coupled system and from information about the remaining part of the structural system, D'Ambrogio and Fregolent [16] identified the dynamic behavior of a structural subsystem. Based on the dual and primal assembly of substructures, de Klerk et. al [17] provided a framework for the various classes of methods and a mathematical description of substructured problems.

The mechanical response of many real-life structural and mechanical systems is restricted by measured response data that can be regarded as constraint conditions. But it is not easy to obtain the exact equilibrium equation of the damaged system because the number of measured data is less than full degrees of freedom. Thus, the response of damaged structural system is predicted by simultaneously solving the static equation at unconstrained state and constraint equations which are measured data.

The static response of damaged system can be described by the external forces as well as the constraint forces to be necessary for obtaining the measured displacement data of damaged system. The damage in a static system induces a loss of structural stiffness and causes variation of the static response. The constraint forces are expressed in terms of the variation of restoring forces which are deeply related with the stiffness.

A truss structure is a structure which consists of axial members connected by pin joints. Thus, each member of the truss structure supports the external load through axial force and it does not undergo the bending deformation. The damage in the truss can not be detected by the existing curvature method or other methods to detect the damage based on flexural response. The damage developed in the truss should be evaluated by the variation of the axial deformation, stress and strain energy.

This study derives a mathematical form to predict the variation in the stiffness matrix diminished by the damage. Based on the variation, the constrained equilibrium equation and constraint forces are explicitly derived. Regarding the stress and strain energy variations caused by the constraint forces as indices to investigate the damage, this work provides an analytical method to detect multiple damages of low damage rate in truss structure using measured data contaminated by noise. It must be effective to reduce the computation time and the number of measurements for investigating substructures that damage is expected rather than the entire system. Partitioning of the damage-expected substructure from an entire structure and using the measured displacements at the boundary, this study presents a method to detect damage in the damage-expected substructure. Numerical applications prove the validity of the proposed method.

2. Formulations for constrained responses of a static system

2.1. Equilibrium equation for the constrained structure

The existence of damage in a static system yields the stiffness change and different response that deviates from the initial one. The stiffness variation requires an updated type of equilibrium equation to satisfy Hooke's law. This section derives the equilibrium equation and constraint forces for the damaged static system from the mathematical form of updated stiffness matrix.

Let us assume that $\mathbf{K}_a$ is an $n \times n$ initial stiffness matrix, $\hat{\mathbf{u}}$ is an $n \times 1$ displacement vector, and $\mathbf{F}$ is an $n \times 1$ given force vector. The equilibrium equation of the system is expressed by:

$$\mathbf{K}_a \hat{\mathbf{u}} = \mathbf{F} \tag{1}$$

The displacements of the initial undamaged system are calculated by:

$$\hat{\mathbf{u}} = \mathbf{K}_a^{-1} \mathbf{F} \tag{2}$$

Assume that the initial system was damaged by external environment and the displacements at m different locations were measured. Thus, the response of the static system is restricted by m measured displacement data expressed as:

$$\mathbf{A}\mathbf{u} = \mathbf{b} \tag{3}$$

where $\mathbf{A}$ is an $m \times n \left(m < n\right)$ Boolean matrix to define the measurement locations, $\mathbf{u}$ is an $n \times 1$ damaged actual response vector and $\mathbf{b}$ indicates the $m \times 1$ vector of measured displacements.

The measured data do not coincide with the solution of the initial equilibrium equation of Eq. (1) and the equilibrium equation of the damaged system should be rewritten by the corrected stiffness matrix $\mathbf{K}$:

$$\mathbf{Ku} = (\mathbf{K}_a + \Delta\mathbf{K})\mathbf{u} = \mathbf{F} \tag{4a}$$

or

$$\mathbf{K}_a\mathbf{u} = \mathbf{F} - \Delta\mathbf{Ku} \tag{4b}$$

where the second term in the right-hand side denotes the constraint forces. The constraint forces are defined as the forces to be required for satisfying the data at measurements.

In practice the number of equations to represent the measurement data of Eq. (3) is less than the number of full degrees of freedom. Therefore the least square method is introduced to describe the damaged displacements and the constraint force vector is derived as a function of the variation in stiffness matrix. They are obtained by minimizing a cost function and deriving the updated stiffness matrix. This study utilizes the cost function written as:

$$J = \frac{1}{2}\left\|\mathbf{K}_a^{1/2}\left(\mathbf{K}^{-1} - \mathbf{K}^{-1}{}_a\right)\mathbf{K}_a^{1/2}\right\| \tag{5}$$

Inserting Eq. (4a) to represent the actual displacement vector into Eq. (3) can be written as:

$$\mathbf{AK}^{-1}\mathbf{F} = \mathbf{b} \tag{6}$$

In order to insert Eq. (6) into Eq. (5), Eq. (6) is modified as follows:

$$\mathbf{AK}_a^{-1/2}\mathbf{K}_a^{1/2}\mathbf{K}^{-1}\mathbf{K}_a^{1/2}\mathbf{K}_a^{-1/2}\mathbf{F} = \mathbf{b} \tag{7}$$

Let $\mathbf{R} = \mathbf{AK}_a^{-1/2}$ and $\mathbf{D} = \mathbf{K}_a^{-1/2}\mathbf{F}$, and solving Eq. (7) with respect to $\mathbf{K}_a^{1/2}\mathbf{K}^{-1}\mathbf{K}_a^{1/2}\mathbf{D}$, we obtain that:

$$\mathbf{K}_a^{1/2}\mathbf{K}^{-1}\mathbf{K}_a^{1/2}\mathbf{D} = \mathbf{R}^+\mathbf{b} + \left(\mathbf{I} - \mathbf{R}^+\mathbf{R}\right)\mathbf{y} \tag{8}$$

where '+' indicates the Moore-Penrose inverse and **y** is an arbitrary vector. Introducing the condition to minimize the cost function of Eq. (5) into Eq. (8) and solving the result with respect to the arbitrary vector, we obtain that:

$$\mathbf{y} = \left(\mathbf{I} - \mathbf{R}^+\mathbf{R}\right)\left(\mathbf{D} - \mathbf{R}^+\mathbf{b}\right) + \mathbf{R}^+\mathbf{Rz} \tag{9}$$

where **z** is an arbitrary vector. Substituting Eq. (9) into Eq. (8), the result can be written as:

$$\mathbf{K}_a^{1/2}\mathbf{K}^{-1}\mathbf{K}_a^{1/2}\mathbf{D} = \mathbf{R}^+\mathbf{b} + \mathbf{D} - \mathbf{R}^+\mathbf{RD} \tag{10}$$

Again, solving Eq. (10) with respect to $\mathbf{K}_a^{1/2}\mathbf{K}^{-1}\mathbf{K}_a^{1/2}$, it follows that:

$$\mathbf{K}_a^{1/2}\mathbf{K}^{-1}\mathbf{K}_a^{1/2} = \left(\mathbf{R}^+\mathbf{b} + \mathbf{D} - \mathbf{R}^+\mathbf{RD}\right)\mathbf{D}^+ + \mathbf{h}\left(\mathbf{I} - \mathbf{DD}^+\right) \tag{11}$$

where **h** is an arbitrary matrix. Using the condition to minimize the cost function of Eq. (5) into Eq. (11) and solving the result with respect to the arbitrary matrix, we obtain that:

$$\mathbf{h} = \left[\mathbf{I} - \left(\mathbf{R}^+\mathbf{b} + \mathbf{D} - \mathbf{R}^+\mathbf{RD}\right)\mathbf{D}^+\right]\left(\mathbf{I} - \mathbf{DD}^+\right) + \mathbf{sDD}^+ \tag{12}$$

where **s** is an arbitrary matrix. The substitution of Eq. (12) into Eq. (11) yields:

$$\mathbf{K}_a^{1/2}\mathbf{K}^{-1}\mathbf{K}_a^{1/2} = \left(\mathbf{R}^+\mathbf{b} - \mathbf{R}^+\mathbf{RD}\right)\mathbf{D}^+ + \mathbf{I} \tag{13}$$

Premultiplying and postmultiplying both sides of Eq. (13) by $\mathbf{K}_a^{-1/2}$, the inverse of the corrected stiffness matrix is expressed as:

$$\mathbf{K}^{-1} = \mathbf{K}_a^{-1} + \mathbf{K}_a^{-1/2}\left(\mathbf{AK}_a^{-1/2}\right)^+\left(\mathbf{b} - \mathbf{A\hat{u}}\right)\left(\mathbf{K}_a^{-1/2}\mathbf{F}\right)^+\mathbf{K}_a^{-1/2} \tag{14}$$

Equation (14) represents the inverse of the corrected stiffness matrix and incorporates the effects of damaged responses. The second term in the right-hand side of Eq. (14) represents the inverse of the stiffness variation. Taking the first-order approximation for obtaining the stiffness matrix from Eq. (14), it yields:

$$\mathbf{K} \approx \mathbf{K}_a + \mathbf{K}_a^{1/2}\left(\mathbf{A}\mathbf{K}_a^{-1/2}\right)^+ \left(\mathbf{b} - \mathbf{A}\hat{\mathbf{u}}\right)\left(\mathbf{K}_a^{-1/2}\mathbf{F}\right)^+ \mathbf{K}_a^{1/2} \tag{15}$$

Thus, the stiffness variation due to damage based on the measured data can be written as:

$$\Delta\mathbf{K} = \mathbf{K}_a^{1/2}\left(\mathbf{A}\mathbf{K}_a^{-1/2}\right)^+ \left(\mathbf{b} - \mathbf{A}\hat{\mathbf{u}}\right)\left(\mathbf{K}_a^{-1/2}\mathbf{F}\right)^+ \mathbf{K}_a^{1/2} \tag{16}$$

Substituting Eq. (15) into Eq. (4a) with the property of $\left(\mathbf{K}_a^{-1/2}\mathbf{F}\right)^+ \mathbf{K}_a^{-1/2}\mathbf{F} = \mathbf{I}$, the static responses of the damaged system are described by:

$$\mathbf{u} = \hat{\mathbf{u}} + \delta\mathbf{u} = \hat{\mathbf{u}} + \mathbf{K}_a^{-1/2}\left(\mathbf{A}\mathbf{K}_a^{-1/2}\right)^+ \left(\mathbf{b} - \mathbf{A}\hat{\mathbf{u}}\right) \tag{17}$$

The second term in the right-hand side of Eq. (17) denotes the displacement variation due to damage. Premultiplying the second term in the right-hand side of Eq. (17) by $\mathbf{K}_a$ the constraint force vector is written as:

$$\mathbf{F}^c = \mathbf{K}_a\left(\delta\mathbf{u}\right) = \mathbf{K}_a^{1/2}\left(\mathbf{A}\mathbf{K}_a^{-1/2}\right)^+ \left(\mathbf{b} - \mathbf{A}\hat{\mathbf{u}}\right) \tag{18}$$

It is observed from Eq. (18) that the constraint forces increase with the increase in the displacement gap between two states at the same position. It means that the response of the system with damage of high level is described by acting high constraint forces on the initial undamaged system. The results of Eqs. (17) and (18) coincide with the ones by Eun et. al [18].

The constraint forces calculated by Eq. (18) exhibit nonzero forces at measurements and zero forces at unmeasurements because they are required for obtaining the measured displacements. Thus, it is difficult to obtain the exact responses at the unmeasured locations by the derived equilibrium equation. It indicates that the responses of damaged system can be more accurately described by increasing the number of measurements to obtain enough information for the damaged system.

The damage existing in the member appears as high stress and strain energy due to the stiffness deterioration. The displacement variation in the damaged system of Eq. (17) is related with the variation in the axial stress and strain energy of truss structure. These variations are calculated by analyzing the truss structure subjected to the external forces as well as the constraint forces. This work considers the variations in the stress and strain energy as indices to evaluate the damage. In the following, we handle two applications to detect damage based on the stress and strain energy variations caused by the constraint forces.

2.2. A three-bay planar truss

As an example to investigate the validity of the proposed method to detect damage based on the variation in stress and strain energy, we consider a three-bay planar truss structure shown in Fig. 1. The truss was modeled by six nodes and ten elements, and the nodal points and the members are numbered as shown in Fig. 1. The truss structure is subjected to the external forces of 100 N in the right direction at the 3$^{\text{th}}$ node and 100 N in the upward direction at the 4$^{\text{th}}$ node. All members have an elastic modulus of 200 GPa and a cross-sectional area of $2.5\times10^{-3}\,\text{m}^2$.

This application considers the truss structure that the strength of the 3$^{\text{th}}$ element is deteriorated by 20 %. We assume that four displacements at nodes 2, 3, 4 and 5 under the action of the external forces were measured as:

$$\begin{bmatrix} u_2 & v_3 & v_4 & u_5 \end{bmatrix}^T = \begin{bmatrix} 0.2 & 1.5 & 2.4 & 0.3 \end{bmatrix}^T \text{mm}$$

where u and v represent the horizontal and vertical displacements at each node, respectively, and the subscript indicates the node number. The measured data are incomplete to investigate the responses of the damaged truss as only 4 of all the 9 degrees of freedom.

Fig. 2 represents the horizontal and vertical components of constraint forces calculated by Eq.

(18). The forces only act on the measured nodes and corresponding directions. The constraint forces are defined as the forces to make up the displacement gap between two states and thus they act only on the measurement locations. The exact displacement or stress variations in the truss structure due to damage are determined by the constraint forces obtained at all degrees of freedom. However, the constraint forces based on the displacement responses measured at several locations provide basic information to obtain the variation of the axial stress and strain energy.

Fig. 3 compares the stress and strain energy variations estimated by Eq. (18) with the actual ones. In the figures, the numerical values represent the absolute values of the stress and strain energy variations between intact and damaged states. It is alluded that the damages exist at the members to exhibit abruptly high stress and strain energy variations due to the loss of stiffness. As presented in the figures, it is determined that the damage is rarely detected based on the stress and strain energy variations because the constraint forces in small truss structure of a few bays are rarely transferred to the other unmeasured members by flexure of upper and lower chords. If the span is longer so that it is affected by the flexural behavior, external forces as well as constraint forces will be transferred along all members. The following application considers a truss structure of long span to investigate that the constraint forces can be properly transferred along the members by flexural behavior.

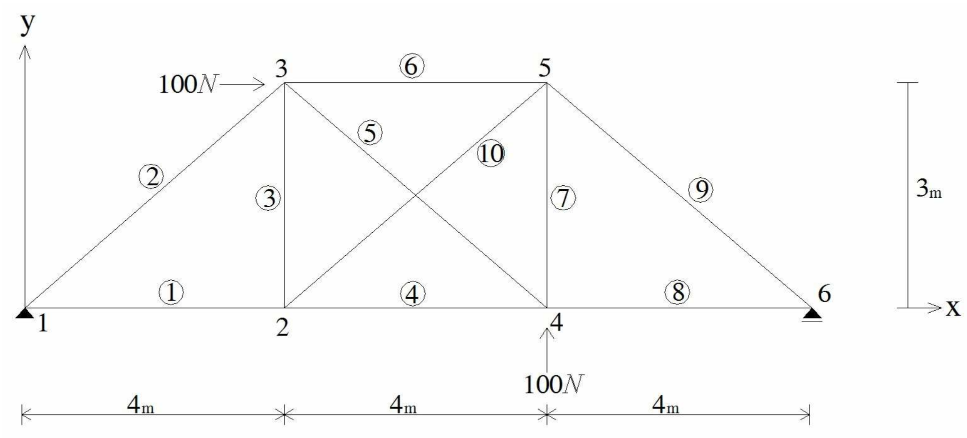

Fig. 1. A three-bay planar truss

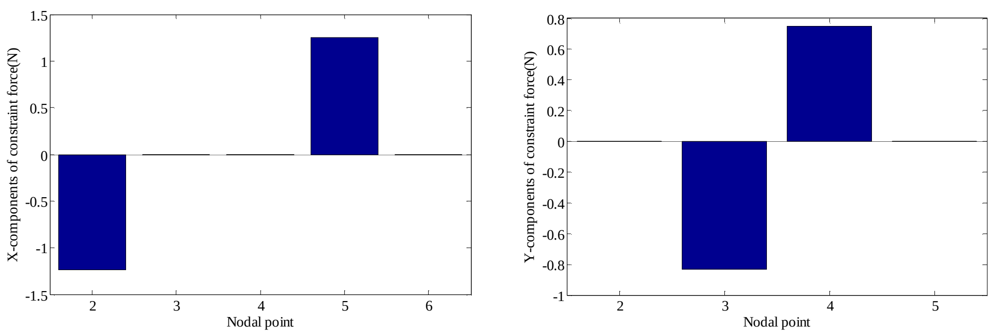

(a) (b)

Fig. 2. Distribution of constraint forces; (a) horizontal components, (b) vertical components

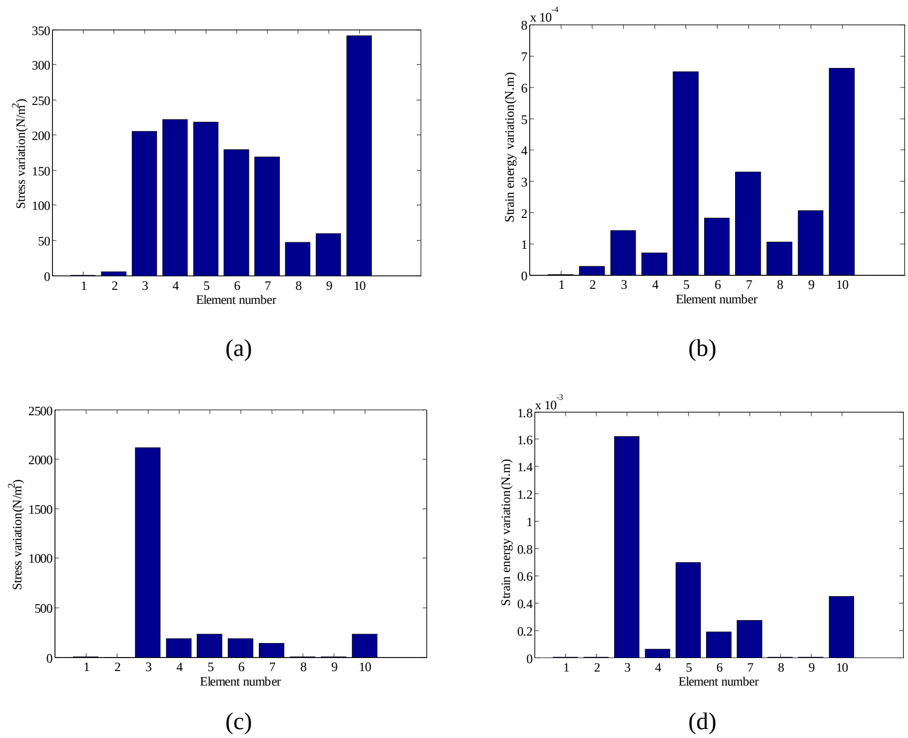

Fig. 3. Stress and strain energy variations of single-damaged three-bay truss; (a) estimated stress variation, (b) estimated strain energy variation, (c) actual stress variation, (d) actual energy strain variation

2.3. An eight-bay planar truss

This application considers the damage detection from the variation in axial stress and strain energy of an eight-bay planar truss structure. The truss has 16 nodes and 35 elements as shown in Fig. 4. The nodal points and the members are numbered as indicated in the figure. The mechanical properties of the truss structure are the same as in the previous truss. We assume that the static displacements were measured as:

$$\begin{aligned}&\begin{bmatrix}u_3 & v_3 & u_5 & v_5 & u_7 & v_7 & u_9 & v_9 & u_{11} & v_{11} & u_{13} & v_{13}\end{bmatrix}^T\\ &=\begin{bmatrix}5.7 & -9.1 & 4.9 & -15.7 & 3.5 & -19.4 & 2.2 & -17.9 & 1.4 & -13.7 & 1.1 & -8.0\end{bmatrix}\text{mm}\end{aligned}$$

The number of measured data is incomplete as only 12 of all the 29 degrees of freedom.

This application considers two cases of two and four damaged members. The damaged members were assumed as 10 % strength reduction. The first case considers the structure of 10 % strength reduction at members 12 and 27. Fig. 5 represents the constraint forces estimated at 12 measurements along upper chord of the truss. The axial stress and strain energy variations caused by the constraint forces are shown in Fig. 6. It is observed from the figures that the damages locate at the members to represent abrupt stress change but the damage can rarely be distinguished from the plot of the variation in the axial strain energy as represented in undamaged member 9 and damaged member 27.

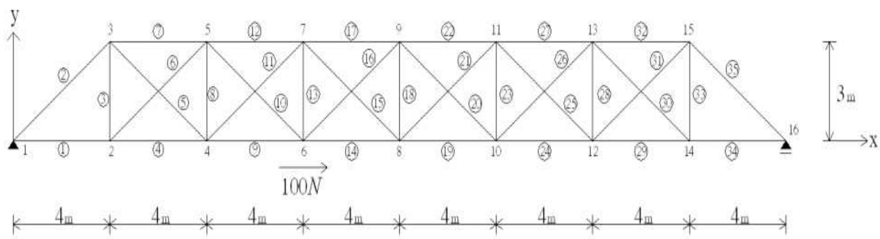

Fig. 4. A eight-bay planar truss

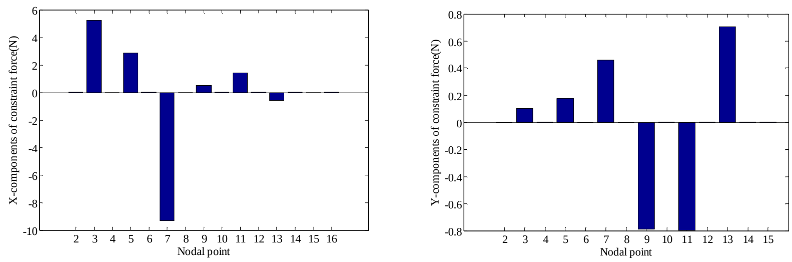

(a) (b)

Fig. 5. Distribution of constraint forces; (a) horizontal components, (b) vertical components

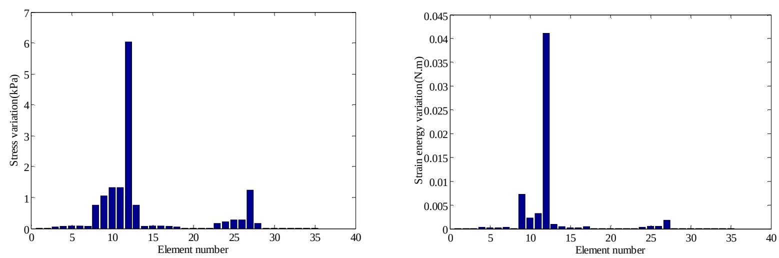

(a) (b)

Fig. 6. Stress and strain energy variations; (a) estimated stress variation, (b) estimated strain energy variation

Fig. 7 represents stress and strain energy variations of the truss structure with four damaged members of 7, 12, 19 and 27 as the second case. It is observed that the damage can be more accurately detected by the stress variation rather than the strain energy variation. The plots indicate that the damage detection at the truss of long span can be accomplished more clearly because the estimated constraint forces are properly transferred on the entire truss structure along all members by flexural behavior.

The effect of the noise included in measured displacement data was investigated. Fig. 8 provides the stress and strain energy variations using measured data contaminated by 5 % noise. It is observed that the noise does rarely affect the proposed detection method. Fig. 9 presents the stress and strain energy variations in the truss structure with 5 % damaged members and 3 % noise. The plots reveal that the damage level is related with the magnitude of stress and strain energy variations but its variation shape is rarely changed. Thus it is demonstrated that the stress variation method can be explicitly utilized regardless of the damage level.

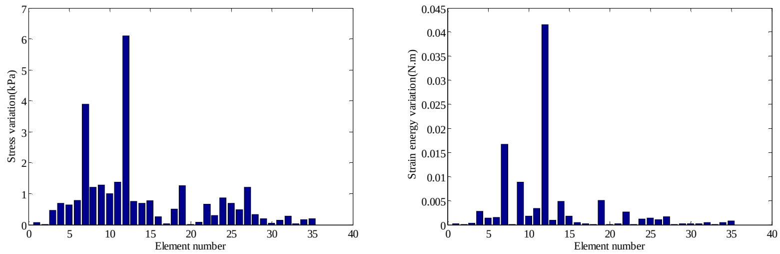

(a) (b)

Fig. 7. Stress and strain energy variations; (a) estimated stress variation, (b) estimated strain energy variation

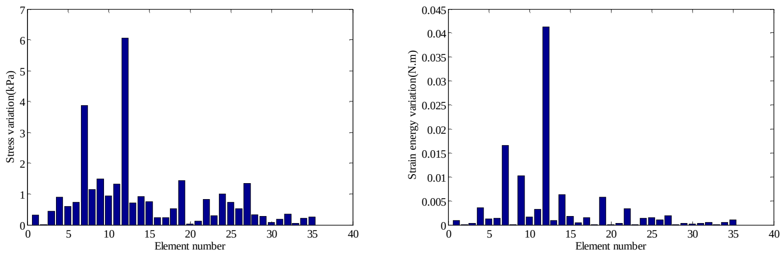

(a) (b)

Fig. 8. Stress and strain energy variations with 5 % noise included in constraint forces; (a) estimated stress variation, (b) estimated strain energy variation

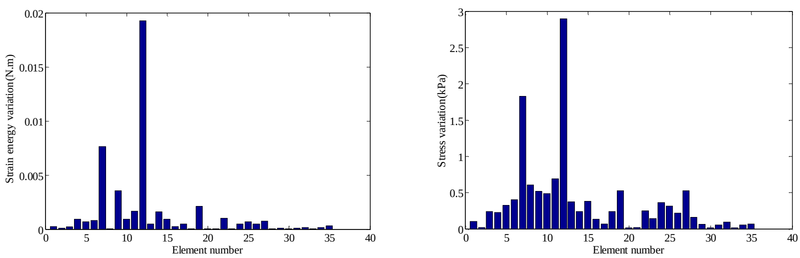

(a) (b)

Fig. 9. Stress and strain energy variations of truss structure of 5 % strength reduction and 3 % noise; (a) estimated stress variation, (b) estimated strain energy variation

3. Analysis of partitioned substructures constrained by the measured data

3.1. Equilibrium equation of the partitioned substructure

Sometimes it can be a tedious process to detect damage from the numerical simulation of finite element model for an entire structure. It would be more effective to locally and precisely investigate the substructures that the damage is expected. This section handles an analytical method to detect the damage in the damage-expected region.

Consider a system to be composed of substructures A and B in Fig. 10. The entire structure has $(n+m)$ degrees of freedom. Partitioning the entire system into two subsystems of A and B, they are expressed by *n* and *m* degrees of freedom, respectively. The static responses at the interface between the substructures A and B, $\mathbf{u}_b^A$ and $\mathbf{u}_b^B$ are described by *r* degrees of freedom and the responses at their interior regions, $\mathbf{u}_i^A$ and $\mathbf{u}_i^B$ are expressed by $(n-r)$ and $(m-r)$ degrees of freedom, respectively. Here, the subscripts i and b denote the interior and boundary regions, respectively. We can assume that the r responses at the boundary between two systems were prescribed by the measured data.

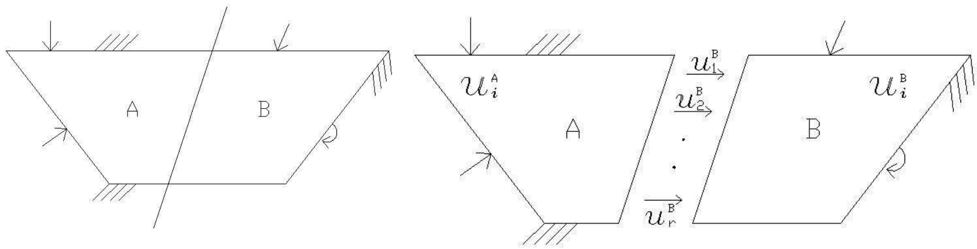

(a) (b)

Fig. 10. Partitioning of an entire structure; (a) entire structure, (b) partitioned substructures

Assuming that damage in the substructure B exists, it is necessary to investigate more precisely the subsystem B for diagnosing the damage. The effects of external loads to act on the substructure A and its physical property should be incorporated in the measured responses at the interface of the partitioned substructure B. That is, it can be interpreted that the substructure is constrained by the prescribed measurements and boundary conditions.

The equilibrium equations of the substructure B can be written as:

$$\begin{bmatrix} \mathbf{K}_{ii}^B & \mathbf{K}_{ib}^B \\ \mathbf{K}_{bi}^B & \mathbf{K}_{bb}^B \end{bmatrix} \begin{bmatrix} \mathbf{u}_i^B \\ \mathbf{u}_b^B \end{bmatrix} = \begin{bmatrix} \mathbf{F}_i^B \\ \mathbf{F}_b^B \end{bmatrix} \tag{19a}$$

or

$$\mathbf{K}^B \mathbf{u}^B = \mathbf{F}^B \tag{19b}$$

where the superscript B denotes the substructure B. Because the boundary responses $\mathbf{u}_b^B$ were measured, the responses in the interior region are calculated by:

$$\mathbf{u}_i^B = \left(\mathbf{K}_{ii}^B\right)^{-1} \left(\mathbf{F}_i^B - \mathbf{K}_{ib}^B \mathbf{u}_b^B\right) \tag{20}$$

where '-1' denotes the inverse and $\mathbf{K}^B$ is the stiffness matrix of full rank.

If the stiffness matrix is not full rank as the floating substructure when the system is partitioned, the structural analysis is performed utilizing the measured data as constraints. Dividing the stiffness matrix of rank deficiency into the diagonal and off-diagonal matrix, $\mathbf{K}_d^B$ and $\mathbf{K}_o^B$, Eq. (19b) can be written as:

$$\mathbf{K}_d^B \mathbf{u}^B = \mathbf{F}^B - \mathbf{K}_o^B \mathbf{u}^B \tag{21}$$

Expressing the measured data in a matrix form like Eq. (3) and substituting its result and Eq. (21) into Eq. (17), the equilibrium equation of the substructure B can be expressed as:

$$\mathbf{u}^B = \left(\mathbf{K}_d^B\right)^{-1} \left(\mathbf{F}^B - \mathbf{K}_o^B \mathbf{u}^B\right) + \left(\mathbf{K}_d^B\right)^{-1/2} \left(\mathbf{A} \mathbf{K}_d^{B^{-1/2}}\right)^+ \left(\mathbf{b} - \mathbf{A}\left(\mathbf{K}_d^B\right)^{-1} \left(\mathbf{F}^B - \mathbf{K}_o^B \mathbf{u}^B\right)\right) \tag{22}$$

And arranging Eq. (22) and solving it with respect to the displacement vector $\mathbf{u}^B$, the responses are expressed as:

$$\mathbf{K}^{B*} \mathbf{u}^B = \mathbf{F}^{B*} \tag{23}$$

where

$$\mathbf{K}^{B*} = \left[\mathbf{I} + \left(\mathbf{K}_d^B\right)^{-1}\mathbf{K}_o^B - \left(\mathbf{K}_d^B\right)^{-1/2}\left(\mathbf{A}\mathbf{K}_d^{B^{-1/2}}\right)^{+}\mathbf{A}\left(\mathbf{K}_d^B\right)^{-1}\mathbf{K}_o^B \right]$$

and

$$\mathbf{F}^{B*} = \left(\mathbf{K}_d^B\right)^{-1}\mathbf{F}^B + \left(\mathbf{K}_d^B\right)^{-1/2}\left(\mathbf{A}\mathbf{K}_d^{B^{-1/2}}\right)^{+}\left(\mathbf{b} - \mathbf{A}\left(\mathbf{K}_d^B\right)^{-1}\mathbf{F}^B\right).$$

The solution of Eq. (23) leads to the response in the interior region to be partitioned without solving the full equilibrium equation on the truss structure. Thus, the derived equation can be easily and effectively utilized in detecting damage in the local region where the damage is expected.

3.2. Damage detection by partitioning eight-bay planar truss

Consider a single-damaged truss structure shown in Fig. 11. The mechanical properties of the truss structure are the same as in the previous truss. Predicting that the damage in the structure exists and partitioning it into two substructures A and B as shown in Fig. 11(a), the damage detection is only performed in the region B of Fig. 11(b) for the damage to be expected. For this numerical simulation, we assume that a damage of 20 % strength reduction locates at element 32 and the responses at 10 locations including the interface indicated in Fig. 11(a) were measured. The measured data are only 10 of all the 29 degrees of freedom and its number was reduced by the partitioning.

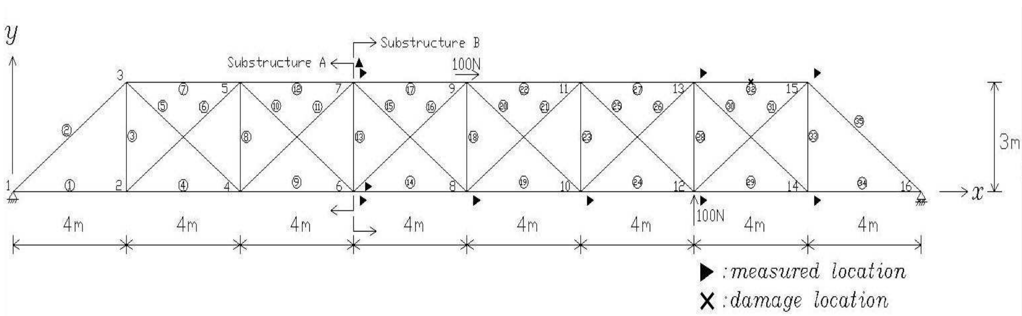

(a)

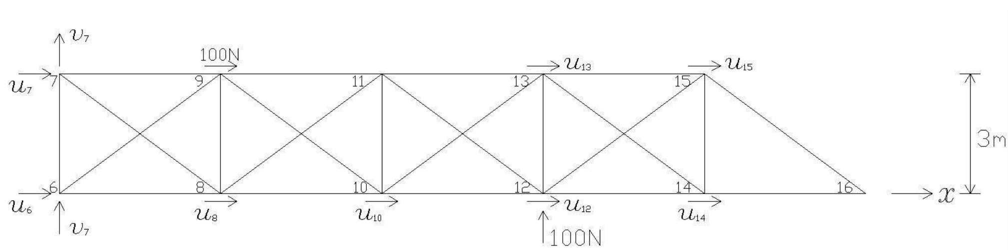

(b)

Fig. 11. A truss structure and partitioning of damaged substructure: (a) an entire truss structure, (b) substructure partitioned by the damage

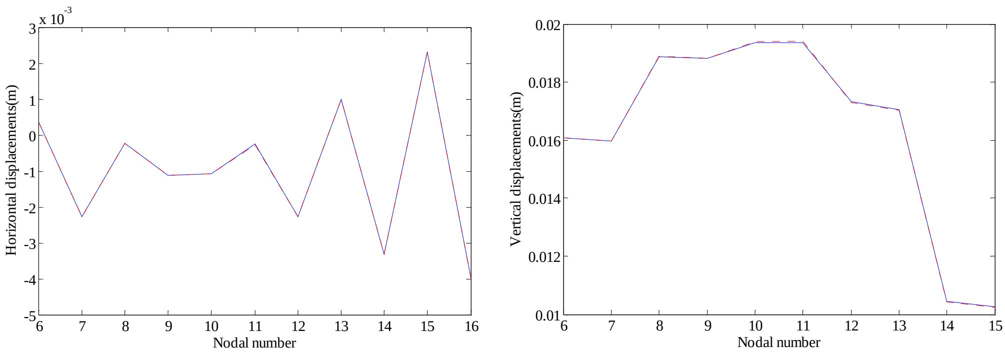

(a) (b)

Fig. 12. Displacement responses by partitioning damaged substructure: (a) horizontal displacements, (b) vertical displacements

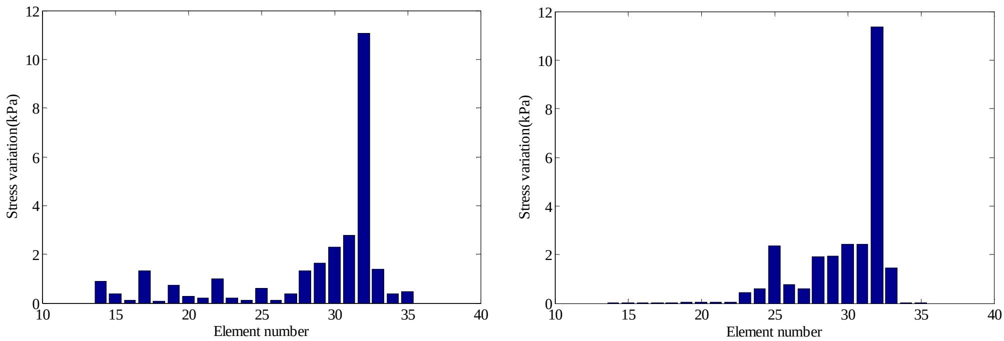

(a) (b)

Fig. 13. Stress variation before and after the damage: (a) estimated stress variation, (b) actual stress variation

Because the stiffness matrix of the partitioned substructure B supported at right end only is rank deficiency, its responses are calculated using Eq. (23) with the measured constraint data. Fig. 12 compares the horizontal and vertical displacements analyzing the entire truss structure and the partitioned substructure. In the figures, it is observed that we cannot find the difference of the displacement responses calculated by both analyses. Determining the internal stresses in the truss member from the calculated displacements, Fig. 13 compares the stress variations in the truss before and after the damage. The damage location can be observed from the stress variation plot. It is observed that the calculated stress variation similarly matches with the actual stress variation. It is expected that the difference between two plots comes from less measurement data than the full number of degrees of freedom. From the application, it is concluded that the partitioning method has merits in reducing the computational time and the measured data as well as enhancing the effectiveness of the damage detection process.

4. Conclusions

The existence of a damage in a system leads to the modification of the stiffness matrix and static equilibrium equation. This work derived a mathematical form on the variation in stiffness matrix of the damaged system, determined the updated equilibrium equation and the constraint forces that are necessary for obtaining the measured displacements. We presented an analytical method to detect damage from the stress and strain energy variations between intact and damage states due to the constraint forces. It was demonstrated that the stress variation could be more accurately utilized as a damage detection criterion than the strain energy, variation could be utilized in detecting the damage of low degree and was rarely affected by external noise. By modifying the derived equation this work proposed a method to detect the damage of the partitioned substructures with stiffness matrix of rank deficiency. The partitioning method enables to reduction of computational time and quantity of the measured data as well as leads to a higher effectiveness of the damage detection. The validity of the proposed method was illustrated by presenting several numerical examples.

Acknowledgement

This research was supported by Basic Science Research Program through the National Research Foundation of Korea (NRF) funded by the Ministry of Education, Science and Technology (no. 2009-0066266).

References

[1] Sheena Z., Unger A., Zalmanovich A. Theoretical stiffness matrix correction by static test results. Israel Journal of Technology 1982;20: 245-253.

[2] Sanayei M., Scampoli S.F. Structural element stiffness identification from static test data. Journal of Engineering Mechanics 1991;117(5): 1021-1036.

[3] Sanayei M., Onipede O. Damage assessment of structures using static test data. AIAA Journal 1991;29(7):1174-1179.

[4] Banan M. R., Banan M. R., Hjelmstad K. D. Parameter estimation of structures from static response. I: Computational aspects. Journal of Structural Engineering 1993;120(11): 3243-3258.

[5] Banan M.R., Banan M.R., Hjelmstad K.D. Parameter estimation of structures from static response. II: Numerical simulation studies. Journal of Structural Engineering 1993;120(11):3259-3283.

[6] Cui F., Yuan W.C., Shi J.J. Damage detection of structures based on static response. Journal of Tongji University 2000;281: 5-8.

[7] Buda G., Caddemi S. Identificatzione del danno di travi di Eulero-Bernoulli soggette a carichi quasi-statici. In: Proceedings of the 16th Aimeta congress, Ferrara, Italy; 2003.

[8] Caddemi S., Greco A. The influence of instrumental errors on the static identification of damage parameters for elastic beams. Computers & Structures 2006;84:1696-1708.

[9] Wang X., Hu N., Fukunaga H., Yao Z.H. Structural damage identification using static test data and changes in frequencies. Engineering Structures 2001;23:610-621.

[10] Bakhtiari-Nejad F., Rahai A., Esfandiari A. A structural damage detection method using static noisy data. Engineering Structures 2005;27:1784-1793.

[11] Caddemi S., Morassi A. Crack detection in elastic beams by static measurements. International Journal of Solids and Structures 2007;44:5301-5315.

[12] Choi I. L., Lee J. S., Choi E., Cho H. N. Development of elastic damage load theorem for damage detection in a statically determinate beam. Computers & Structures 2004;82:2483-2492.

[13] Escobar J.A., Sosa J. J., Gomez R. Structural damage detection using the transformation matrix. Computers & Structures 2005:83;357-368.

[14] Rodriguez R., Escobar J.A., Gomez R. Damage location and assessment along structural elements using damage submatrices. Engineering Structures 2009:31;475-486.

[15] Ozen G. O., Kim J. H. Direct identification and expansion of damping matrix for experimental-analytical hybrid modeling. Journal of Sound and Vibration 2007; 308: 348-372.

[16] D'Ambrogio W., Fregolent A. The role of interface DoFs in decoupling of substructures based on the dual domain decomposition. Mechanical Systems and Signal Processing 2010; 24: 2035-2048.

[17] de Klerk D., Rixen D.J., Voormeeren S. N. General framework for dynamic substructuring: History, review, and classification of techniques. AIAA Joural 2008; 46(5): 1169-1181.

[18] Eun H. C., Lee E. T., Chung H. S. On the static analysis of constrained structural systems. Canadian Journal of Civil Engineering 2004;31:1119-1122.